SARS-CoV-2 Omicron-specific mRNA vaccine induces potent and broad antibody responses in vivo

Zhenhao Fang [1,2,3,*], Lei Peng [1,2,3,*],
Qianqian Lin [1,2,3], Ping Ren [1,2,3], Kazushi Suzuki [1,2,3], Qiancheng Xiong [6,7,8],
Paul Clark [1,2,3], Chenxiang Lin [6,7,8], and Sidi Chen [1,2,3,4,5,9,10,11,@,#]

Affiliations

1. Department of Genetics, Yale University School of Medicine, New Haven, CT, USA
2. System Biology Institute, Yale University, West Haven, CT, USA
3. Center for Cancer Systems Biology, Yale University, West Haven, CT, USA
4. Molecular Cell Biology, Genetics, and Development Program, Yale University, New Haven, CT, USA
5. Immunobiology Program, Yale University, New Haven, CT, USA
6. Department of Cell Biology, Yale University, New Haven, CT, USA
7. Department of Biomedical Engineering, Yale University, New Haven, CT, USA
8. Nanobiology Institute, Yale University, New Haven, CT, USA
9. Comprehensive Cancer Center, Yale University School of Medicine, New Haven, CT, USA
10. Stem Cell Center, Yale University School of Medicine, New Haven, CT, USA
11. Center for Biomedical Data Science, Yale University School of Medicine, New Haven, CT, USA

* Co-first authors.

@ Correspondence:

SC (sidi.chen@yale.edu)

Lead contact:

SC (sidi.chen@yale.edu)

+1-203-737-3825 (office)

+1-203-737-4952 (lab)

Abstract

The Omicron variant of SARS-CoV-2 has high transmissibility and recently been sweeping the globe, dominating new infection cases in the US and many regions in the world. Due to its extensive number of mutations, this variant has high level of immune evasion, which drastically reduced the efficacy of existing antibodies and vaccines. Thus, it is important to develop an Omicron-specific vaccine and test if it can induce immune responses against Omicron and broadly against other variants. Here, we generated an Omicron-specific lipid nanoparticle (LNP) mRNA vaccine candidate, and tested its potency of antibody induction in animals, both alone and as a booster to existing mRNA vaccine designed against the ancestral reference virus (WA-1). This Omicron-specific LNP-mRNA vaccine elicited strong and specific antibody response in vaccination-naïve mice. Consistent with recent reports, mice that received two-dose WA-1 LNP-mRNA, the one mimicking the commonly used Pfizer/Moderna mRNA vaccine administered in the general population, showed a 41-fold reduction in neutralization potency against Omicron variant as compared to WA-1 two weeks post second dose, which further reduced to background level 3.5 months post second dose. As a booster for WA-1 mRNA vaccination, a single dose Omicron LNP-mRNA induced potent antibody response against the Omicron variant, with over 1,000-fold increase at two weeks post injection as compared to the blood samples right before booster. The Omicron-specific antibody level of the Omicron-boosted samples is numerically similar to WA-1 vaccine against WA-1 variant. This boost also elicited broader antibody responses against WA-1 and Delta variants, restoring these activities of the WA-1 vaccinated animals that also dropped over time. A consecutive second dose of Omicron LNP-mRNA 2 weeks following the first dose did not significantly increased the level of antibodies. These *in vivo* animal data provided a timely proof-of-concept for Omicron-specific mRNA vaccination, alone and as a booster to the existing widely-used mRNA vaccine form.

Key words

Omicron variant, mRNA vaccine, Omicron-specific mRNA vaccine, COVID-19, SARS-CoV-2, lipid nanoparticle (LNP), neutralizing antibody, waning immunity, Omicron booster shots

Introduction

Since its first identification in specimen collected in November 2021[1], the Omicron variant (B.1.1.529) of SARS-CoV-2 has been rapidly spreading across the globe, reported in many countries and regions[2-5]. The Omicron variant was associated with increased risk of reinfection according to a population-level evidence in South Africa[6]. Two days after its initial report to World Health Organization (WHO), Omicron was designated as a variant of concern (VoC) by WHO on November 26[7]. Population-level data indicated that Omicron has become the dominant variant in South Africa in mid-November[8], only one week after the first traceable case. Similarly in January 2022, Omicron variant has dominated newly diagnosed cases in many states of the US[9], Canada[10] and UK[4]. Omicron variant has started to drive the fourth wave of COVID-19 in South Africa[11] and around the world[12]. Its case doubling time is faster than previous waves[12], hinting its increased transmissibility and/or immune evasion. A number of urgent questions on Omicron have quickly become central concerns, which include whether Omicron can evade immunity from therapeutic antibodies, past infection or vaccination, whether Omicron-caused disease is more severe or infectious, and whether and when Omicron-specific vaccine or antibody will be available against Omicron variant.

Mounting clinical and laboratory evidence have shown that most of therapeutic and natural antibodies for COVID-19 failed to retain potency against Omicron variant[13-18]. The Omicron variant has 60 mutations compared to the ancestral variant's reference sequence (also referred to as prototypic virus / variant, reference, wildtype (WT), Wuhan-1, or WA-1)[5]. There are 50 nonsynonymous, 8 synonymous, and 2 non-coding mutations, of which many are not observed in any other variants. There are a total of 32 mutations in the spike protein, which is the main antigen target of therapeutic antibodies and of many widely administered vaccines, including 30 amino acid changes, three small deletions, and one small insertion, of which 15 are within the receptor-binding domain (RBD)[19]. Due to its extensive number of mutations, this variant has high level of immune evasion, which drastically reduced the efficacy of existing antibodies and vaccines. Omicron spike mutations are concerning as they cluster on known neutralizing antibody epitopes[15] and some of them have well-characterized consequences such as immune evasion and higher infectivity. In fact, recent reports showed that the vast majority of the existing monoclonal antibodies developed against SARS-CoV-2 have dramatic reduction in effectiveness against the

95 Omicron variant[13-18], leading to recall or exclusion of recommended use of certain therapeutic
96 antibodies under emergency authorization[20].
97
98 The mRNA vaccine has achieved immense success in curbing the viral spread and reducing the
99 risk of hospitalization and death of COVID-19, for the past variants[21,22]. However, a significant
100 drop of mRNA vaccine's effectiveness against Omicron has been reported from clinical[8] and
101 laboratory studies of samples of vaccinated individuals[23,24]. In light of the heavily altered antigen
102 landscape of Omicron spike, assessing the efficacy of Omicron-specific mRNA vaccine is urgently
103 needed. However, to date, there is no clinical or preclinical data of Omicron-specific mRNA
104 vaccine publicly available. A number of critical questions regarding Omicron-specific mRNA
105 vaccine need to be addressed. For examples: What is the immunogenicity of Omicron spike used
106 in a vaccine form? Whether potent antibody immunity can be induced by an Omicron-specific
107 mRNA vaccine, and how well does that neutralize the Omicron variant? If, and how, does the
108 immune response induced by the Omicron-specific mRNA vaccine react to other variants, such as
109 WA1 or Delta? Finally, because a large existing population in the world received authorized
110 Pfizer/BioNTech or Moderna mRNA vaccines that encodes the reference (WA-1) spike antigen,
111 it is important to know whether an Omicron mRNA vaccine can boost the reduced or waning
112 immunity associated with this existing vaccination.
113
114 To answer some of these questions, we directly generated an Omicron-specific lipid nanoparticle
115 (LNP) mRNA vaccine candidate that encodes an engineered full-length Omicron spike with
116 HexaPro mutations, and evaluated its effect alone, and as booster shots after SARS-CoV-2 WA-1
117 mRNA vaccine *in vivo* in animal models.
118
119
120 **Results**
121 **Design, generation and physical characterization of an Omicron-specific LNP-mRNA**
122 **vaccine candidate**
123 We designed an Omicron-specific LNP-mRNA vaccine candidate based on the full-length spike
124 sequence of the Omicron variant from two North America patients identified on Nov23rd, 2021.
125 The spike coding sequence of WA-1 and Omicron variant was flanked by 5' UTR, 3' UTR and 3'

126 PolyA tail (**Figure 1A**). Six Proline mutations (HexaPro) were introduced to spike sequence, as
127 they were reported to improve spike protein stability and prefusion state [25]. The furin cleave site
128 (RRAR) in spike was replaced with GSAS stretch to keep integrity of S1 and S2 unit. We then
129 encapsulated the transcribed spike mRNA into lipid nanoparticles to produce WA-1 and Omicron
130 LNP-mRNAs, and characterized the quality and biophysical properties by downstream assays
131 including dynamic light scattering, transmission electron microscope and receptor binding assay.
132
133 The dynamic light scattering and transmission electron microscope were applied to evaluate the
134 size distribution and shape of Omicron LNP-mRNA, which showed a monodispersed sphere shape
135 with an average radius of 52 nm and polydispersity index of 0.17 (**Figure 1C-1E**). To evaluate the
136 effectiveness of LNP-mRNA mediated Omicron spike expression in cells as well as the receptor
137 binding ability of the designed Omicron HexaPro spike, Omicron LNP-mRNA was directly added
138 to HEK293T cells 16 hours before subjecting cells to flow cytometry. Evident surface expression
139 of functional Omicron HexaPro spike capable of binding to hACE2 was observed by staining cells
140 with human ACE2-Fc fusion protein and PE anti-Fc secondary antibody (**Figure 1F**). These data
141 showed that the Omicron spike sequence was successfully encoded into an mRNA, encapsulated
142 into the LNP, can be introduced into mammalian cells efficiently without additional manipulation,
143 and express functional spike protein that binds to human ACE2.
144
145 **Specific binding and neutralizing antibody response elicited by Omicron LNP-mRNA**
146 **against the Omicron variant**
147 After ensuring functional spike expression mediated by Omicron LNP-mRNA, we proceeded to
148 characterizing the immunogenicity of Omicron LNP-mRNA *in vivo*. In order to test rapid immune
149 elicitation against Omicron variant, we performed the following vaccination and testing schedule.
150 Two doses of 10 μg Omicron LNP-mRNA, as prime and boost two weeks apart were
151 intramuscularly injected into five C57BL/6Ncr (B6) mice (Figure 1G). Retro-orbital blood was
152 collected prior to immunization on day 0, 13 and 21, i.e. two weeks post prime (one day before
153 boost), and one week post boost. We then isolated plasma from blood, which was used in ELISA
154 and neutralization assay to quantify binding and neutralizing antibody titers. A significant increase
155 in antibody titers against Omicron spike RBD was observed in ELISA assay from plasma samples

156 post prime and boost (**Figure 1H-1I**). These data showed that the Omicron LNP-mRNA induced
157 strong and specific antibody responses in vaccinated mice *in vivo*.
158
159 **Omicron LNP-mRNA boosted waning immunity of WA-1 LNP-mRNA immunized mice**
160 In light of the wide coverage of the ancestral WA-1-based LNP-mRNA vaccine (to model those
161 widely administered in the current general population), we sought to test: (i) the effect of WA-1
162 LNP-mRNA vaccination against Omicron variant, (ii) the immunity induced by WA-1 LNP-
163 mRNA over time, and (iii) whether Omicron LNP-mRNA could boost the waning immunity
164 against Omicron variant, WA-1 and/or Delta variant. To gain initial answers to these questions in
165 animal models, we sequentially vaccinated B6 mice with two doses of WA-1 and Omicron LNP-
166 mRNA with a 106-day interval between last dose of WA-1 and first dose of Omicron LNP-mRNA
167 (**Figure 2A**). We collected blood samples of these animals in a rational time series, including day
168 35 (2 weeks post two doses of WA-1 LNP-mRNA vaccination), day 127 (3.5 months post two
169 doses of WA-1 LNP-mRNA vaccination, immediately before Omicron LNP-mRNA vaccination),
170 day 140 (~2 weeks post the first booster dose of Omicron LNP-mRNA vaccination, one day before
171 the second Omicron dose), and day 148 (1 week post two doses of Omicron LNP-mRNA
172 vaccination).
173
174 Plasma samples were purified from blood samples and analyzed in ELISA and neutralization
175 assays against SARS-CoV-2 Omicron, Delta or WA-1. Comparing to the titers against WA-1 and
176 Delta RBD, the binding antibody titers against Omicron RBD elicited by WA-1 mRNA-LNP were
177 significantly weaker in samples from both day 35 and 127 (**Figures 2B and S1**). The group average
178 Omicron RBD reactivity is 20 fold (day 35) and 11 fold (day 127) lower than that of WA-1 RBD,
179 and 18 fold (day 35) and 10 fold (day 127) lower than Delta (**Figure S2**). A steep drop (two to
180 three orders of magnitude) of antibody titers from mice immunized with WA-1 LNP-mRNA was
181 observed after three months (day 35 vs. day 127) from all three RBD datasets. It is worth noting
182 that the antibody titers on day 127 (3.5 months post WA-1 boost, prior to Omicron booster)
183 decreased to a level that is near-baseline (PBS controls), particularly for titers against Omicron
184 RBD.
185

186 A single dose of Omicron LNP-mRNA booster shot drastically increased the antibody titers of
187 mice vaccinated with WA-1 LNP-mRNA, by over 2,000 fold as compared to the sample right
188 before boost (**Figure 2B**), which reached a level numerically comparable to the post-boost titer by
189 Omicron LNP-mRNA alone (**Figure 1I)**. Interestingly, the Omicron LNP-mRNA shot boosted not
190 only titers against Omicron RBD, but also titers against Delta and WA-1 RBD, although the extent
191 of titer increase was more drastic in the Omicron RBD data (**Figure 2B**). The antibody titers did
192 not increase one week after a second boost of Omicron LNP-mRNA.

193

194 Because pseudovirus neutralization is a relatively safer and widely-used assay that strongly
195 correlates with live virus results and has been regarded as a standard proxy by the field [24,26-28], we
196 set out to use pseudovirus neutralization assay to measure the neutralizing antibody responses
197 induced by Omicron LNP-mRNA booster in these animals. We first generated HIV-1 based
198 Omicron pseudovirus system. Interestingly, we found that under exactly the same virus production
199 and assay conditions, the Omicron pseudovirus has substantially higher infectivity than both WA-
200 1 (8x increase) and Delta (4x) pseudoviruses (**Figure S3A-C**), consistent with its higher infectivity
201 reported previously[24,29,30]. We then normalized the pseudoviruses by functional titers (number of
202 infected cells / volume), and used this system to perform pseudovirus neutralization assays on all
203 the plasma samples collected (**Figure S3D**). The neutralization results showed a consistent overall
204 pattern as ELISA results, with a striking contrast among titers against Omicron pseudovirus
205 (**Figure 2C**). On day 35 and 127, the mice post boost of WA-1 LNP-mRNA showed significantly
206 lower neutralizing antibody titers against Omicron variant than titers against Delta variant or WA-
207 1 (**Figure S4**). For the samples two weeks post boost (day 35), the group average Omicron RBD
208 neutralization reactivity is 41 fold lower than that of WA-1 RBD, and 11 fold lower than Delta.
209 When comparing samples collected on day 35 and 127, around two orders of magnitude (10s~100s
210 of fold change) time-dependent titer reduction was unequivocally observed in all three pseudovirus
211 neutralization data (**Figure 2C**). The Omicron-neutralization activity of WA-1 vaccinated mice
212 3.5 months post boost (day 127) was as low as undetectable (**Figure 2C**). These data suggested
213 that there was severe waning antibody immunity in the standard two-dose WA-1 vaccinated
214 animals, which completely lost neutralization ability against the Omicron variant pseudovirus.
215

216 A single booster shot of Omicron LNP-mRNA vaccine drastically enhanced the antibody titers
217 against Omicron variant two weeks after the injection, of which the surge was over 1000-fold (log
218 IC50 changed from below 0.5 to nearly 4) (**Figure 2C**). The neutralizing titer after this surge by
219 Omicron vaccine surpassed the titer two weeks post WA-1 vaccine boost (day 35). Interestingly,
220 the Omicron mRNA vaccine also rescued the antibody titers against Delta and WA-1
221 pseudoviruses, with a two orders of magnitude increase in both ELISA titers and neutralization
222 activity (**Figure 2B-2C**). A second booster shot two weeks after the first of Omicron mRNA
223 vaccine yielded little increase in titers or neutralization activity against Omicron, WA-1 or Delta
224 variants at the time measured (day 148, 1 week after the second dose) (**Figure 2C**). Overall, the
225 ELISA titers and neutralization activity significantly correlated with each other across all samples
226 and animals tested (**Figure 2D**). These data suggested that a single dose Omicron LNP-mRNA
227 induced potent antibody response against the Omicron variant, along with broader activity against
228 the ancestral WA-1 and the recent Delta variant, in mouse models at the timepoints measured.
229

230 **Discussion**

231 The rapid spread of Omicron variant around the world, especially in countries with wide coverage
232 of vaccines designed based on the ancestral antigen (e.g. WA-1 mRNA vaccine), is particularly
233 concerning. The extensive mutations in Omicron spike mark a dramatic alteration in its
234 antigenicity[15]. Omicron variant has high transmissibility and high level of immune evasion from
235 WA-1 mRNA vaccine induced immunity, which was reported from various emerging literature
236 [6,14-17]. Omicron's strong association with reinfection[6] or breakthrough infection[8,12] and its heavily
237 altered antigenicity prompted the idea of developing Omicron-specific mRNA vaccine.
238

239 In this study, we generated a HexaPro-version Omicron spike LNP-mRNA vaccine candidate. In
240 mouse models, we validated that it can induce potent Omicron-specific antibody response, and
241 tested its boosting effect to animals previously received two-dose WA-1 mRNA vaccine shots. An
242 encouraging observation is that potent antibody immunity can be achieved by a single dose of
243 Omicron LNP-mRNA. The titer of single dose Omicron LNP-mRNA vaccinated mouse plasma
244 was numerically similar to the antibody titer against Omicron observed 2 weeks post boost of WA-
245 1 LNP-mRNA (log10 AUC around 3 in **Figure 1I and 2B**), although it is still unclear whether the
246 potency of the Omicron mRNA vaccine is associated with the high number of mutations of the

247 antigen. Because of the high starting titers post prime, the titer change post boost by Omicron
248 LNP-mRNA was less prominent (**Figure 1I**).
249
250 To date (as of Jan 9, 2022), 4.6 billion people, i.e. 60% of the global population, received COVID-
251 19 vaccination (Our World in Data[31]). Almost all those vaccines were designed based on the
252 antigen from the ancestral virus, including the two approved mRNA vaccine BNT162b2 [21] and
253 mRNA-1273 [22], both of which were based on the reference / WA-1 spike sequence. Individuals
254 receiving existing vaccines have waning immunity overtime, reported for multiple approved or
255 authorized vaccines including the two mRNA vaccines[32-35]. Thus, it is important to test the effect
256 of Omicron-specific vaccine candidate as booster shots in the context of WA-1 mRNA vaccine.
257
258 Consistent with past reports, we observed a dramatic time-dependent decrease (around 100-fold
259 decrease) of binding and neutralizing antibody titers against Omicron, Delta variants and WA-1
260 strain 3.5 months after the second dose of WA-1 mRNA vaccine. This observed waning immunity
261 is particularly concerning in the scenario of rapid spreading of Omicron variant, which largely
262 escapes the humoral immune response elicited by WA-1 mRNA vaccines as evident in published
263 studies[14-16,18] as well as in our current data. While a limitation of our study is that these are animal
264 data, although the antibody responses to vaccination is highly conserved between mouse and
265 human (and that the mouse is a widely used preclinical model by major vaccine makers[36,37]). In
266 fact, a very recent report showed waning immunity in vaccinated individuals[24] and that a booster
267 shot using the original WA-1 based mRNA vaccine helps recover partial immunity. However, the
268 neutralizing antibody titers even after the boost with a WA-1 based vaccine titer were still
269 significantly lower against Omicron as compared to WA-1 and other variants, urging for
270 development and testing of an Omicron-specific vaccine not studied before.
271
272 We tested the Omicron-specific LNP-mRNA vaccine candidate in the context of WA-1 vaccinated
273 animals. While animals almost completely lost antibody protection against Omicron even though
274 they received two doses of WA-1 mRNA vaccine 3.5 months ago, our results showed that a single
275 dose of Omicron mRNA vaccination boosted neutralizing antibody titers over 1000-fold against
276 Omicron. In addition, the Omicron-specific vaccine also brought back neutralizing titers against
277 WA-1 and Delta variants to a level comparable to peak titers by WA-1 mRNA vaccine. The

278 Omicron booster shot provided superior protection against Omicron variant and comparable
279 humoral defense against WA-1 and Delta variants. Such surge of antibody titer by Omicron booster
280 shot, and the neutralization activities against WA-1 and Delta, two of the once-dominant variants,
281 suggest that the Omicron-specific LNP-mRNA can provide broader activities, and may therefore
282 be worth considering over the WA-1 LNP-mRNA booster. These animal model results provided
283 timely initial data in reference for further development of Omicron-specific vaccine and potential
284 testing as a booster.
285

Acknowledgments

We thank various members from our labs for discussions and support. We thank staffs from various Yale core facilities (Keck, YCGA, HPC, YARC, CBDS and others) for technical support. We thank Drs. Tsemperouli, Karatekin, and others for providing equipment and related support. We thank various support from Department of Genetics; Institutes of Systems Biology and Cancer Biology; Dean's Office of Yale School of Medicine and the Office of Vice Provost for Research.

Funding

This work is supported by DoD PRMRP IIAR (W81XWH-21-1-0019) and discretionary funds to SC. The TEM core is supported by NIH grant GM132114 to CL.

Institutional Approval

This study has received institutional regulatory approval. All recombinant DNA (rDNA) and biosafety work were performed under the guidelines of Yale Environment, Health and Safety (EHS) Committee with approved protocols (Chen 18-45, 20-18, 20-26). All animal work was performed under the guidelines of Yale University Institutional Animal Care and Use Committee (IACUC) with approved protocols (Chen-2020-20358; Chen 2021-20068).

305 **Figure legends**

306 **Figure 1. Omicron-specific LNP-mRNA vaccine elicited binding antibodies against SARS-**
307 **CoV-2 Omicron variant**.

308 **A**, Illustration of mRNA vaccine construct expressing SARS-CoV-2 WA-1 and Omicron spikes.
309 The spike open reading frame were flanked by 5' untranslated region (UTR), 3' UTR and polyA
310 tail. The Omicron mutations (red) and HexaPro mutations (black) were numbered based on WA-
311 1 spike residue number.

312 **B**, Distribution of Omicron spike mutations (magenta) were displayed in one protomer of spike
313 trimer of which NTD, RBD, hinge region and S2 were colored in purple, blue, green and orange
314 respectively (PDB: 7SBL). The HexaPro mutations in S2 were colored in cyan.

315 **C**, Schematics illustrating the formulation and biophysical characterization of LNP-mRNA.

316 **D**, Dynamic light scattering derived histogram depicting the particle radius distribution of Omicron
317 spike LNP-mRNA.

318 **E**, Omicron LNP-mRNA image collected on transmission electron microscope.

319 **F**, human ACE2 receptor binding of LNP-mRNA encoding Omicron spike expressed in 293T cells
320 as detected by human ACE2-Fc fusion protein and PE-anti-human Fc antibody on Flow cytometry.

321 **G**, Immunization and sample collection schedule. Retro-orbital blood were collected prior
322 Omicron LNP-mRNA vaccination on day 0, day 13 and day 21. Five mice (n=5) were
323 intramuscularly injected with 10 μg Omicron LNP-mRNA on day 0 (prime, Omicron x 1) and day
324 14 (boost, Omicron x 2). The plasma and peripheral blood mononuclear cells (PBMCs) were
325 separated from blood for downstream assays. The slight offset of the labels reflects the fact that
326 each of the blood collections were perform prior to the vaccination injections.

327 **H**, ELISA titration curves over serial $\log_{10}$-transformed dilution points of plasma collected from
328 mice before and after immunization with Omicron LNP-mRNA at defined time points.

329 **I**, Binding antibody titers of plasma from mice vaccinated with Omicron LNP-mRNA against
330 Omicron spike RBD as quantified by area under curve of $\log_{10}$-transformed titration curve (Log_{10}
331 AUC) in Figure 1H. Each dot in bar graphs represents value from one mouse.

332 Data on dot-bar plots are shown as mean ± s.e.m. with individual data points in plots. One-way
333 ANOVA with Tukey's multiple comparisons test was used to assess statistical significance.
334 Statistical significance labels: * $p < 0.05$; ** $p < 0.01$; *** $p < 0.001$; **** $p < 0.0001$. Non-
335 significant comparisons are not shown, unless otherwise noted as n.s., not significant.

336

337 **Figure 2. Omicron specific LNP-mRNA booster shots greatly improved waning immunity of**
338 **mice vaccinated with SARS-CoV-2 WA-1 LNP-mRNA against both SARS-CoV-2 Delta and**
339 **Omicron variants.**

340 **A**, Schematics showing the immunization and blood sampling schedule of mice (n=3) administered
341 with 1 μg WA-1 LNP-mRNA prime (WA-1 x 1) and boost (WA-1 x 2) as well as additional 10 μg
342 Omicron-specific LNP-mRNA booster shots. The plasma and PBMCs were separate from blood
343 for downstream assays. The slight offset of the labels reflects the fact that each of the blood
344 collections were perform prior to the vaccination injections.

345 **B**, Bar graph comparing binding antibody titers of mice administered with PBS or WA-1 and
346 Omicron LNP-mRNA against Omicron, Delta and WA-1 RBD (ELISA antigens). The antibody
347 titers were quantified as area under curve of $\log_{10}$-transformed titration curve (Log_{10} AUC) in
348 Extended Data Figure 1. PBS sub-groups (n=3 each) collected from different matched time points
349 showed no statistical differences between each other, and were combined as one group (n=12).

350 **C**, Neutralizing antibody titers in the form of $\log_{10}$-transformed reciprocal IC50 calculated from
351 fitting the titration curve with a logistic regression model.

352 **D**, Correlation of neutralization titers ($\log_{10}$ reciprocal IC50, y axis) and ELISA titers ($\log_{10}$ AUC,
353 x axis) from matched vaccination group (left panel) or individual mouse (right panel). PBS samples
354 from different timepoints were shown as one group in correlation map and were not included in
355 linear regression model. Each dot in bar graphs represents value from one group average (left
356 panel), or one individual mouse (right panel).

357 Data on dot-bar plots are shown as mean ± s.e.m. with individual data points in plots. Two-way
358 ANOVA with Tukey's multiple comparisons test was used to assess statistical significance.
359 Statistical significance labels: * $p < 0.05$; ** $p < 0.01$; *** $p < 0.001$; **** $p < 0.0001$. Non-
360 significant comparisons are not shown, unless otherwise noted as n.s., not significant.

361

362

363 **Extended Data Figures**

364 **Extended Data Figure 1 (Figure S1). ELISA titration curves over serial dilution of plasma**
365 **collected at different timepoints from mice administered with PBS or WA-1 and/or Omicron**
366 **LNP-mRNA**.

367 ELISA curves of serial log_{10}-transformed dilution points of plasma collected from mice before and
368 after immunization with Omicron LNP-mRNA, against spike receptor binding domain (RBD)
369 antigens of Omicron variant (left), Delta (mid) and WA-1 (right) were shown.

370

371 **Extended Data Figure 2 (Figure S2). Binding antibody titers of mice administered with PBS**
372 **or WA-1 and Omicron LNP-mRNA against Omicron, Delta and WA-1 RBD (ELISA**
373 **antigens), were grouped by vaccination timepoints to compare titers against different RBD**
374 **antigens.** The antibody titers were quantified as area under curve of log_{10}-transformed titration
375 curve (Log_{10} AUC) in Extended Data Figure 1.

376

377 **Extended Data Figure 3 (Figure S3). Omicron, Delta and WA-1 pseudovirus production,**
378 **characterization and neutralization assay.**

379 **A.** Functional titration curves of Omicron, Delta and WA-1 pseudoviruses in hACE2+ cells.

380 **B.** Representative Flow Cytometry plots of infectivity of Omicron, Delta and WA-1 pseudoviruses
381 in hACE2+ cells.

382 **C.** Quantification of infectivity of Omicron, Delta and WA-1 pseudoviruses in hACE2+ cells.

383 **D.** Neutralization titration curves of plasma from mice administered with PBS or WA-1 and
384 Omicron LNP-mRNA against Omicron (left), Delta (mid) and WA-1 (right) pseudovirus.
385 Pseudovirus infection rate was calculated from percent of GFP positive cells and was plotted
386 against plasma dilution (log_{10} transformed) as titration curve.

387

388 **Extended Data Figure 4 (Figure S4). Neutralizing antibody titers in the form of log_{10}-**
389 **transformed reciprocal IC50 were grouped by vaccination timepoints to compare titers**
390 **against different pseudoviruses.** The neutralization titers were quantified as log_{10}-transformed
391 reciprocal IC50 values (Log_{10} reciprocal IC50, or Log_{10} IC50,) in Extended Data Figure 3.

392

393 **Extended Data Figure 5 (Figure S5). Representative flow cytometry gating strategy for**
394 **detecting Omicron spike binding to human ACE2 receptor.**
395
396

397 **Methods**

398 **Molecular cloning**

399 The Omicron spike amino acid sequence was derived from two Omicron cases identified in Canada
400 on Nov.23rd, 2021 (EpiCoV, EPI_ISL_6826713 and EPI_ISL_6826714). Omicron spike cDNA
401 were codon optimized, synthesized as gblocks (IDT) and cloned to mRNA vector with 5', 3'
402 untranslated region (UTR) and poly A tail. The furin cleave site (RRAR) was replaced with a
403 GSAS short stretch in the mRNA vector. HexaPro mutations were introduced in the WA-1 and
404 Omicron variant spike sequence of mRNA vector to improve expression and prefusion state[25]. The
405 accessory plasmids for pseudovirus assay including pHIVNLGagPol and pCCNanoLuc2AEGFP
406 were from Dr. Bieniasz' lab[38]. The C-terminal 19 amino acids were deleted in the SARS-CoV-2
407 spike sequence for the pseudovirus assay.

408

409 **Cell Culture**

410 HEK293T, HEK293FT (Thermo Fisher) and 293T-hACE2 (gifted from Dr Bieniasz' lab) cell lines
411 were maintained in Dulbecco's modified Eagle's medium (DMEM, Thermo fisher) supplemented
412 with 10% Fetal bovine serum (Hyclone) and 1% penicillin-streptomycin (Gibco), which is denoted
413 as complete growth medium. Cells were split every 2 days at a split ratio of 1:4 when the
414 confluency reached over 80%.

415

416 **In vitro mRNA transcription and vaccine formulation**

417 A Hiscribe™ T7 ARCA mRNA Kit (with tailing) (NEB, Cat # E2060S) was used to in vitro
418 transcribe codon-optimized mRNA encoding HexaPro spikes of SARS-CoV-2 WT and Omicron
419 variant with 50% replacement of uridine by N1-methyl-pseudouridine. The DNA template was
420 linearized before mRNA transcription and contained 5′ UTR, 3′ UTR and 3′ polyA tail as
421 flanking sequence of spike open reading frame.

422

423 The purified mRNA was generated by following NEB manufacturer's instructions and kept frozen
424 at -80 °C until further use. The lipid nanoparticles mRNA was assembled using the
425 NanoAssemblr® Ignite™ instrument (Precision Nanosystems) according to manufacturers'
426 guidance. In brief, lipid mixture was mixed with prepared mRNA in 25mM sodium acetate at pH
427 5.2 on Ignite instrument at a molar ratio of 6:1 (LNP : mRNA), similar to previously described[36,39].

428 The LNP encapsulated mRNA (LNP-mRNA) was buffer exchanged to PBS using 100kDa Amicon
429 filter (Macrosep Centrifugal Devices 100K, 89131-992). Sucrose was added as a cryoprotectant.
430 The particle size of mRNA-LNP was determined by DLS device (DynaPro NanoStar, Wyatt,
431 WDPN-06) and TEM described below. The encapsulation rate and mRNA concentration were
432 quantified by Quant-iT™ RiboGreen™ RNA Assay (Thermo Fisher).
433

434 **Validation of LNP-mRNA mediated spike expression in vitro and receptor binding**
435 **capability of expressed Omicron HexaPro spikes**

436 On day 1, HEK293T cells were seeded at 50% confluence in 24-well plate and mixed with 2 μg
437 Omicron LNP-mRNA. After 16 hours, the cells were collected for flow cytometry. The spike
438 expression on cell surface were detected by staining cells with human ACE2–Fc chimera (Sino
439 Biological, 10108-H02HG) in MACS buffer (D-PBS with 2 mM EDTA and 0.5% BSA) for 20
440 min on ice. Cells were washed twice after the primary stain and incubated with PE–anti-human Fc
441 antibody (Biolegend, 410708) in MACS buffer for 20 min on ice. During secondary antibody
442 staining, live/Dead aqua fixable stain (Invitrogen) was used to assess cell viability. Data was
443 collected on BD FACSAria II Cell Sorter (BD) and analyzed using FlowJo software.
444

445 **Negative-stain TEM**

446 Formvar/carbon-coated copper grid (Electron Microscopy Sciences, catalog number FCF400-Cu-
447 50) was glow-discharged and covered with 6 μl of the sample for 1 min before blotting away the
448 sample. The sample was double-stained with 6 μl of 2% (w/v) uranyl formate (Electron
449 Microscopy Sciences, catalog number 22450) for 5 seconds (first stain) and 1 min (second stain),
450 blotting away after each stain. Images were collected using a JEOL JEM-1400 Plus microscope
451 with an acceleration voltage of 80 kV and a bottom-mount charge-coupled device camera (4k by
452 3k, Advanced Microscopy Technologies).
453

454 **Mouse vaccination**

455 Vaccine immunogenicity study used 6 weeks old female C57BL/6Ncr (B6) mice purchased from
456 Charles River. The mice-housing condition was maintained at regular ambient room temperature
457 (65-75°F, or 18-23°C), 40-60% humidity, and a 14 h:10 h day/night cycle. Each mice cage was
458 individually ventilated with clean food, water, and bedding. Two sets of immunization experiments

459 were performed: vaccination with Omicron LNP-mRNA, and sequential vaccination with WA-1
460 and Omicron LNP mRNA. For the Omicron LNP-mRNA vaccination experiment, five mice were
461 immunized with 10 µg Omicron LNP-mRNA on day 0 (prime) and day 14 (boost). Retro-orbital
462 blood was collected prior to vaccine injection on day 0, day 13 and day 21. For WA-1 and Omicron
463 LNP-mRNA sequential vaccination experiment, three mice were administered with either 100 µl
464 PBS or two-dose 1 µg WA-1 (21 days apart) and 10 µg Omicron LNP-mRNA (14 days apart).
465 Retro-orbital blood was collected prior to vaccine injection on day 35, day 127, day 140 and day
466 148.
467

468 **Isolation of plasma and PBMCs from blood**

469 At the defined time points, retro-orbital blood was collected from mice. The isolation of PBMCs
470 and plasma was achieved via centrifugation using SepMate-15 and Lymphoprep gradient medium
471 (StemCell Technologies). 200 µl blood was immediately diluted with 800 µl PBS with 2% FBS.
472 The blood diluent was then added to SepMate-15 tubes with 6ml Lymphoprep (StemCell
473 Technologies). Centrifugation at 1200 g for 20 minutes was used to isolate RBCs, PBMCs and
474 plasma. 250ul diluted plasma was collected from the surface layer. The remaining solution at the
475 top layer was poured to a new tube to isolate PBMCs, which were washed once with PBS + 2%
476 FBS. The separated plasma was used in ELISA and neutralization assay. And PBMCs were kept
477 frozen for future use.
478

479 **ELISA**

480 3 µg/ml of spike antigens were coated onto the 384-well ELISA plates (VWR, Cat # 82051-300)
481 overnight at 4 degree. The antigen panel used in the ELISA assay includes RBDs of 2019-nCoV
482 WA-1 (Sino Biological 40592-V08B), Delta variant B.1.617.2 (Sino Biological 40592-V08H90)
483 and Omicron variant B.1.1.529 (Sino Biological 40592-V08H121). Plates were washed with PBST
484 (PBS plus 0.5% Tween 20) three times in the 50TS microplate washer (Fisher Scientific,
485 NC0611021) and blocked with 0.5% BSA in PBST at room temperature for one hour. Plasma was
486 fourfold serially diluted starting at a 1:500 dilution. Diluted plasma samples were added to the
487 plates and incubated at room temperature for one hour, followed by washes with PBST five times.
488 Anti-mouse secondary antibody (Fisher, Cat# A-10677) at 1:2500 dilution in blocking buffer was
489 incubated at room temperature for one hour. Plates were washed five times and developed with

490 tetramethylbenzidine substrate (Biolegend, 421101). The reaction was stopped with 1 M
491 phosphoric acid after 20 min at room temperature, and OD at 450 nm was measured by multimode
492 microplate reader (PerkinElmer EnVision 2105). The binding response (OD450) was plotted
493 against the dilution factor in log10 scale as the dilution-dependent response curve. The area under
494 curve of the dilution-dependent response (Log10 AUC) was calculated to quantify the potency of
495 the plasma antibody binding to spike antigens. The fold change of antibody titer was estimated
496 using this equation: fold change = 10 ^ (AUC1 - AUC2)
497

498 **Omicron, WA-1 and Delta pseudovirus production and characterization**

499 For the neutralization assay, HIV-1 based SARS-CoV-2 WT, B.1.617.2 (Delta) variant, and
500 B.1.1.529 (Omicron) variant pseudotyped virions were packaged using a coronavirus spike
501 plasmid, a reporter vector and a HIV-1 structural protein expression plasmid. The reporter vector,
502 pCCNanoLuc2AEGFP, and plasmid expressing HIV-1 structural proteins (pHIVNLGagPol) were
503 gifts from Dr Bieniasz's lab. The spike plasmid for SARS-CoV-2 WA-1 pseudovirus truncated C-
504 terminal 19 amino acids (denoted as SARS-CoV-2-Δ19) and was from Dr Bieniasz' lab. Spike
505 plasmids expressing C-terminally truncated SARS-CoV-2 B.1.617.2 variant S protein (Delta
506 variant-Δ19) and SARS-CoV-2 B.1.1.529 variant S protein (Omicron variant-Δ19) were made
507 based on the pSARS-CoV-2-Δ19. All pseudoviruses were produced under the same conditions.
508 Briefly, 293FT cells were seeded in 150 mm plates, and transfected with 21 µg pHIVNLGagPol,
509 21 µg pCCNanoLuc2AEGFP, and 7.5 µg of corresponding plasmids, in the presence of 198 µl
510 PEI (1mg/ml, PEI MAX, Polyscience). At 48 h after transfection, the supernatant was filtered
511 through a 0.45-µm filter, and frozen in -80°C.
512

513 To characterize the tilter of WA-1, Delta, and Omicron pseudoviruses packaged, 0.01 x10^6 293T-
514 hACE2 cells were plated in each well of a 96-well plate. In the next day, different volumes of
515 pseudovirus supplemented with culture medium to a total volue of 100 µL were added into 96-
516 well plates with 293T-hACE2. Plates were incubated at 37°C for 24 hr. Then cells were washed
517 with MACS buffer once and the percent of GFP-positive cells were counted by Attune NxT
518 Acoustic Focusing Cytometer (Thermo Fisher). To normalize pseudovirus tilter, 0.01 x10^6 293T-
519 hACE2 cells were plated in each well of a 96-well plate. In the next day, 50 µL pseudovirus was
520 mixed with 50 µL culture medium to 100 µL. The mixture was incubated for 1 hr in the 37 °C

521 incubator, supplied with 5% CO2, and added into 96-well plates with 293T-hACE2. Plates were
522 incubated at 37°C for 24 hr. Then cells were washed with MACS buffer once and the percent of
523 GFP-positive cells were counted by Attune NxT Acoustic Focusing Cytometer (Thermo Fisher).
524 Delta pseudovirus and Omicron pseudovirus were diluted accordingly to match the functional tilter
525 of WA-1 pseudovirus for neutralization assay of plasma samples.
526
527 **Pseudovirus neutralization assay**
528 The SARS-CoV-2 pseudovirus assays were performed on 293T-hACE2 cells. One day before
529 infection, 0.01 x10^6 293T-hACE2 cells were plated in each well of a 96-well plate. In the next day,
530 plasma collected from mice were serially diluted by 5 fold with complete growth medium at a
531 starting dilution of 1:100. 55 μL diluted plasma was mixed with the same volume of SARS-CoV-
532 2 WA-1, Delta variant, or Omicron variant pseudovirus and was incubated for 1 hr in the 37 °C
533 incubator, supplied with 5% CO2. 100 μL of mixtures were added into 96-well plates with 293T-
534 hACE2. Plates were incubated at 37°C for 24 hr. Then cells were washed with MACS buffer once
535 and the percent of GFP-positive cells were counted by Attune NxT Acoustic Focusing Cytometer
536 (Thermo Fisher). The 50% inhibitory concentration (IC50) was calculated with a four-parameter
537 logistic regression using GraphPad Prism (GraphPad Software Inc.). If the fitting value of IC50 is
538 negative (i.e. negative titer), which suggested undetectable neutralization activity, the value was
539 set to baseline (1, 0 in log scale).
540
541 **Standard statistics**
542 Standard statistical methods were applied to non-high-throughput experimental data. The
543 statistical methods are described in figure legends and/or supplementary Excel tables. The
544 statistical significance was labeled as follows: n.s., not significant; * $p < 0.05$; ** $p < 0.01$; *** p
545 < 0.001; **** $p < 0.0001$. Prism (GraphPad Software) and RStudio were used for these analyses.
546 Additional information can be found in the supplemental excel tables.
547
548 **Schematic illustrations**
549 Schematic illustrations were created with Affinity Designer or BioRender.
550
551 **Replication, randomization, blinding and reagent validations**

552 Biological or technical replicate samples were randomized where appropriate. In animal
553 experiments, mice were randomized by littermates.
554 Experiments were not blinded.
555 Commercial antibodies were validated by the vendors, and re-validated in house as appropriate.
556 Custom antibodies were validated by specific antibody - antigen interaction assays, such as ELISA.
557 Isotype controls were used for antibody validations.
558 Cell lines were authenticated by original vendors, and re-validated in lab as appropriate.
559 All cell lines tested negative for mycoplasma.
560

561 **Data, resources and code availability**

562 All data generated or analyzed during this study are included in this article and its supplementary
563 information files. Specifically, source data and statistics for non-high-throughput experiments are
564 provided in a supplementary table excel file. Additional information related to this study are
565 available from the corresponding author(s) upon reasonable request.
566

567 **References**

568

569 1 *Science Brief: Omicron (B.1.1.529) Variant*, <https://www.cdc.gov/coronavirus/2019-
570 ncov/science/science-briefs/scientific-brief-omicron-variant.html#1> (

571 2 Khare, S. *et al.* GISAID's Role in Pandemic Response. *China CDC Wkly* **3**, 1049-1051,
572 doi:10.46234/ccdcw2021.255 (2021).

573 3 *Omicron daily overview: 31 December 2021*,
574 <https://assets.publishing.service.gov.uk/government/uploads/system/uploads/attachment
575 _data/file/1044522/20211231_OS_Daily_Omicron_Overview.pdf> (

576 4 *Omicron cases tracker by Newsnodes*, <https://newsnodes.com/nu_tracker> (

577 5 *Tracking Omicron variant, GISAID*, <https://www.gisaid.org/hcov19-variants/> (

578 6 Pulliam, J., et al. Increased risk of SARS-CoV-2 reinfection associated with emergence
579 of the Omicron variant in South Africa. *MedRxiv*,
580 doi:https://doi.org/10.1101/2021.11.11.21266068 (2021).

581 7 *Classification of Omicron (B.1.1.529): SARS-CoV-2 Variant of Concern*,
582 <https://www.who.int/news/item/26-11-2021-classification-of-omicron-(b.1.1.529)-sars-
583 cov-2-variant-of-concern> (

584 8 Collie, S., Champion, J., Moultrie, H., Bekker, L. G. & Gray, G. Effectiveness of
585 BNT162b2 Vaccine against Omicron Variant in South Africa. *N Engl J Med*,
586 doi:10.1056/NEJMc2119270 (2021).

587 9 *SARS-CoV-2 Omicron variant: statistics*, <https://en.wikipedia.org/wiki/SARS-CoV-
588 2_Omicron_variant#Epidemiology> (

589 10 *Tracking variants of the novel coronavirus in Canada*,
590 <https://www.ctvnews.ca/health/coronavirus/tracking-variants-of-the-novel-coronavirus-
591 in-canada-1.5296141> (

592 11 Viana, R., et al. Rapid epidemic expansion of the SARS-CoV-2 Omicron variant in
593 southern Africa. *Nature*, doi:https://www.nature.com/articles/d41586-021-03832-5.

594 12 Karim, S. S. A. & Karim, Q. A. Omicron SARS-CoV-2 variant: a new chapter in the
595 COVID-19 pandemic. *Lancet* **398**, 2126-2128, doi:10.1016/S0140-6736(21)02758-6
596 (2021).

13 Kozlov, M. Omicron overpowers key COVID antibody treatments in early tests. *Nature*, doi:10.1038/d41586-021-03829-0 (2021).

14 Cameroni, E. *et al.* Broadly neutralizing antibodies overcome SARS-CoV-2 Omicron antigenic shift. *bioRxiv*, doi:10.1101/2021.12.12.472269 (2021).

15 Cao, Y., et al. Omicron escapes the majority of existing SARS-CoV-2 neutralizing antibodies. *Nature*, doi:https://doi.org/10.1038/d41586-021-03796-6 (2021).

16 Planas, D., et al. Considerable escape of SARS-CoV-2 variant Omicron to antibody neutralization. *Nature*, doi:https://doi.org/10.1038/d41586-021-03827-2 (2021).

17 Aggarwal, A., et al. SARS-CoV-2 Omicron: evasion of potent humoral responses and resistance to clinical immunotherapeutics relative to viral variants of concern. *MedRxiv*, doi:https://doi.org/10.1101/2021.12.14.21267772 (2021).

18 Hoffmann, M., et al. The Omicron variant is highly resistant against antibody-mediated neutralization – implications for control of the COVID-19 pandemic. *Cell*, doi:https://doi.org/10.1016/j.cell.2021.12.032 (2021).

19 *Implications of the emergence and spread of the SARS-CoV-2 B.1.1. 529 variant of concern (Omicron) for the EU/EEA*, <https://www.ecdc.europa.eu/sites/default/files/documents/Implications-emergence-spread-SARS-CoV-2%20B.1.1.529-variant-concern-Omicron-for-the-EU-EEA-Nov2021.pdf> (

20 *U.S. Pauses Distribution Of Monoclonal Antibody Treatments That Proved Ineffective Against Omicron*, <https://www.forbes.com/sites/zacharysmith/2021/12/23/us-pauses-distribution-of-monoclonal-antibody-treatments-that-proved-ineffective-against-omicron/?sh=57bf26bf4c62> (

21 Polack, F. P. *et al.* Safety and Efficacy of the BNT162b2 mRNA Covid-19 Vaccine. *N Engl J Med* **383**, 2603-2615, doi:10.1056/NEJMoa2034577 (2020).

22 Baden, L. R. *et al.* Efficacy and Safety of the mRNA-1273 SARS-CoV-2 Vaccine. *N Engl J Med* **384**, 403-416, doi:10.1056/NEJMoa2035389 (2021).

23 Cele, S. *et al.* SARS-CoV-2 Omicron has extensive but incomplete escape of Pfizer BNT162b2 elicited neutralization and requires ACE2 for infection. *medRxiv*, doi:10.1101/2021.12.08.21267417 (2021).

24 Garcia-Beltran, W. F. *et al.* mRNA-based COVID-19 vaccine boosters induce neutralizing immunity against SARS-CoV-2 Omicron variant. *Cell*, doi:10.1016/j.cell.2021.12.033 (2022).

25 Hsieh, C. L. *et al.* Structure-based design of prefusion-stabilized SARS-CoV-2 spikes. *Science* **369**, 1501-1505, doi:10.1126/science.abd0826 (2020).

26 Bewley, K. R. *et al.* Quantification of SARS-CoV-2 neutralizing antibody by wild-type plaque reduction neutralization, microneutralization and pseudotyped virus neutralization assays. *Nat Protoc* **16**, 3114-3140, doi:10.1038/s41596-021-00536-y (2021).

27 Nie, J. *et al.* Quantification of SARS-CoV-2 neutralizing antibody by a pseudotyped virus-based assay. *Nat Protoc* **15**, 3699-3715, doi:10.1038/s41596-020-0394-5 (2020).

28 Liu, L. *et al.* Potent neutralizing antibodies against multiple epitopes on SARS-CoV-2 spike. *Nature* **584**, 450-456, doi:10.1038/s41586-020-2571-7 (2020).

29 Luo, C. H., et al. Infection with the SARS-CoV-2 Delta Variant is Associated with Higher Infectious Virus Loads Compared to the Alpha Variant in both Unvaccinated and Vaccinated Individuals. *medRxiv*, doi:https://doi.org/10.1101/2021.08.15.21262077.

30 Liu, Y. & Rocklov, J. The reproductive number of the Delta variant of SARS-CoV-2 is far higher compared to the ancestral SARS-CoV-2 virus. *J Travel Med* **28**, doi:10.1093/jtm/taab124 (2021).

31 *Coronavirus (COVID-19) Vaccinations*, <https://ourworldindata.org/covid-vaccinations?country=OWID_WRL> (

32 Goldberg, Y. *et al.* Waning Immunity after the BNT162b2 Vaccine in Israel. *N Engl J Med* **385**, e85, doi:10.1056/NEJMoa2114228 (2021).

33 Thomas, S. J. *et al.* Safety and Efficacy of the BNT162b2 mRNA Covid-19 Vaccine through 6 Months. *N Engl J Med* **385**, 1761-1773, doi:10.1056/NEJMoa2110345 (2021).

34 Levin, E. G. *et al.* Waning Immune Humoral Response to BNT162b2 Covid-19 Vaccine over 6 Months. *N Engl J Med* **385**, e84, doi:10.1056/NEJMoa2114583 (2021).

35 Doria-Rose, N. *et al.* Antibody Persistence through 6 Months after the Second Dose of mRNA-1273 Vaccine for Covid-19. *N Engl J Med* **384**, 2259-2261, doi:10.1056/NEJMc2103916 (2021).

36 Corbett, K. S. *et al.* SARS-CoV-2 mRNA vaccine design enabled by prototype pathogen preparedness. *Nature* **586**, 567-571, doi:10.1038/s41586-020-2622-0 (2020).

658 37 Vogel, A. B., et al. A prefusion SARS-CoV-2 spike RNA vaccine is highly immunogenic
659 and prevents lung infection in non-human primates. *bioRxiv*,
660 doi:https://doi.org/10.1101/2020.09.08.280818 (2020).

661 38 Schmidt, F. *et al.* Measuring SARS-CoV-2 neutralizing antibody activity using
662 pseudotyped and chimeric viruses. *J Exp Med* **217**, doi:10.1084/jem.20201181 (2020).

663 39 Hassett, K. J. *et al.* Optimization of Lipid Nanoparticles for Intramuscular Administration
664 of mRNA Vaccines. *Mol Ther Nucleic Acids* **15**, 1-11, doi:10.1016/j.omtn.2019.01.013
665 (2019).

666

Figure 1

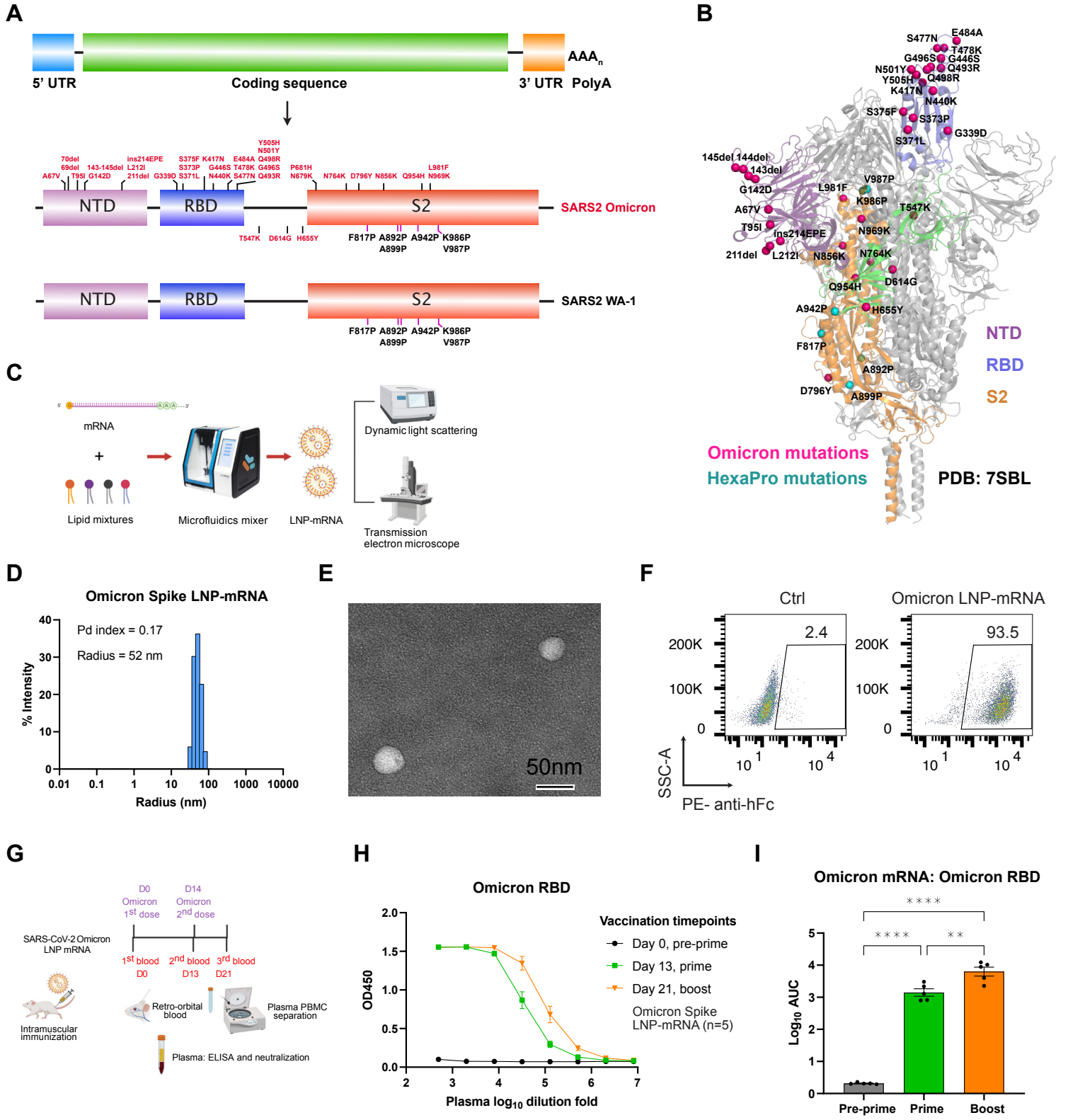
A
5' UTR
Coding sequence
3' UTR
PolyA
AAA$_n$
NTD
RBD
S2
SARS2 Omicron
SARS2 WA-1
B
Omicron mutations
HexaPro mutations
PDB: 7SBL
NTD
RBD
S2
C
mRNA
Lipid mixtures
Microfluidics mixer
LNP-mRNA
Dynamic light scattering
Transmission electron microscope
D
Omicron Spike LNP-mRNA
Pd index = 0.17
Radius = 52 nm
% Intensity
Radius (nm)
E
50nm
F
Ctrl
Omicron LNP-mRNA
2.4
93.5
SSC-A
PE- anti-hFc
G
SARS-CoV-2 Omicron LNP mRNA
D0 Omicron 1st dose
D14 Omicron 2nd dose
1st blood D0
2nd blood D13
3rd blood D21
Intramuscular immunization
Retro-orbital blood
Plasma PBMC separation
Plasma: ELISA and neutralization
H
Omicron RBD
OD450
Plasma log10 dilution fold
Vaccination timepoints
Day 0, pre-prime
Day 13, prime
Day 21, boost
Omicron Spike LNP-mRNA (n=5)
I
Omicron mRNA: Omicron RBD
Log10 AUC
Pre-prime
Prime
Boost

Figure 2

A

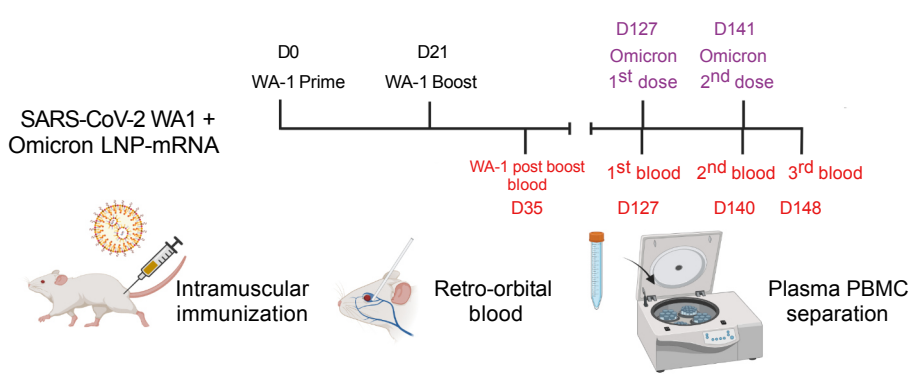

B

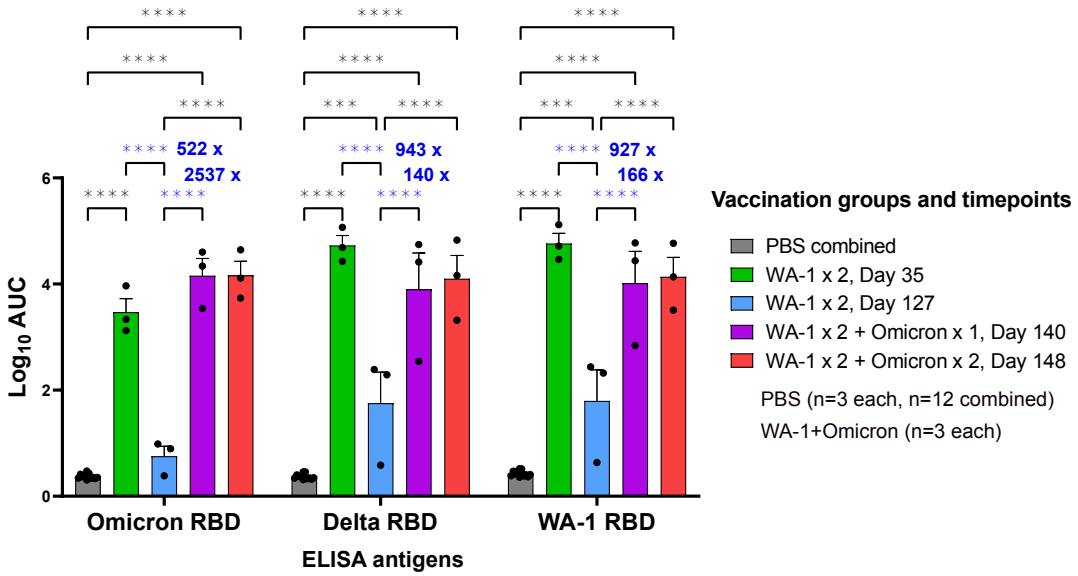

C

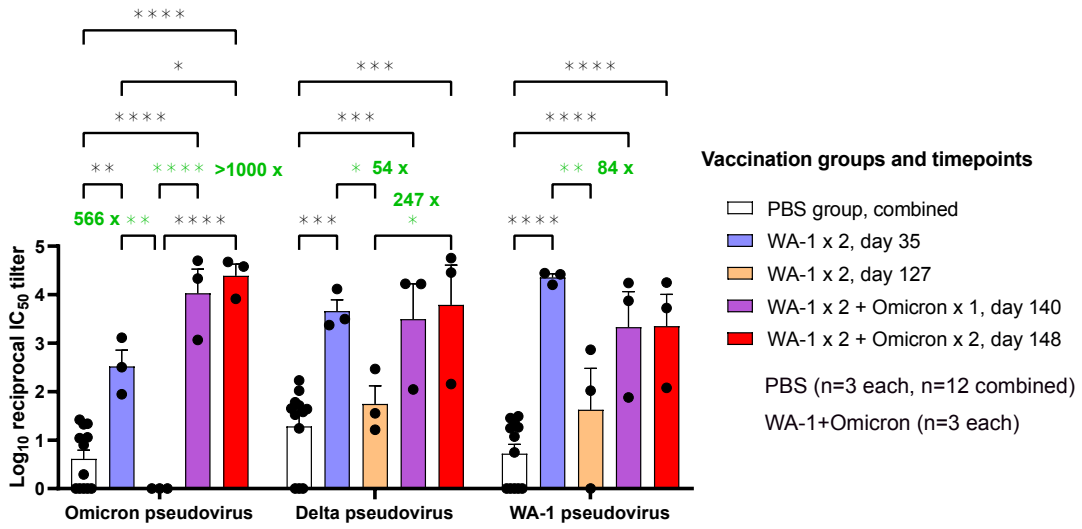

D

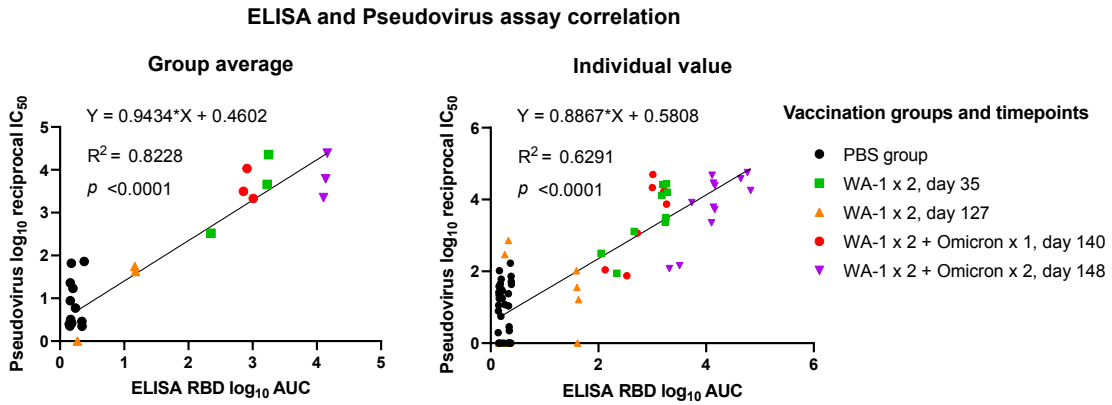

Figure S1

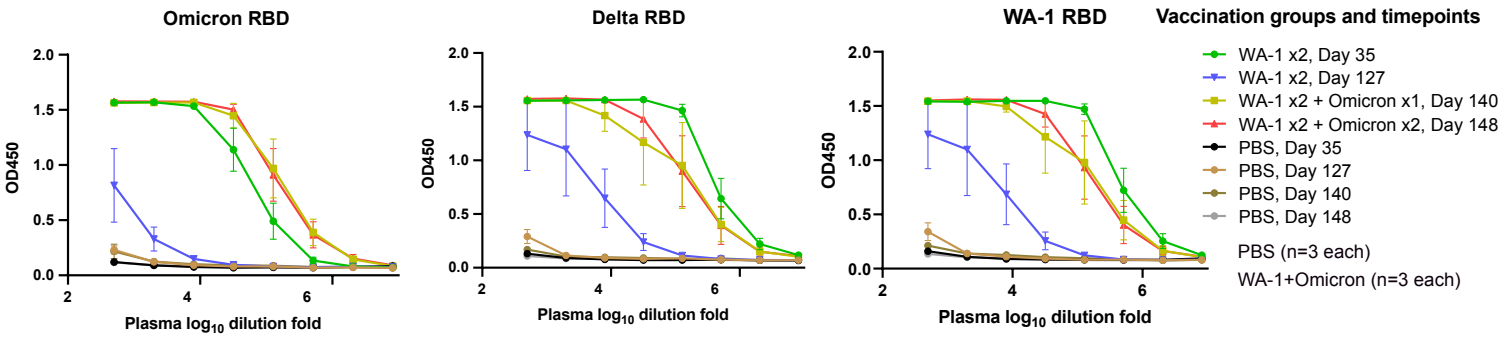
Omicron RBD
Delta RBD
WA-1 RBD
OD450
2.0
1.5
1.0
0.5
0.0
2
4
6
Plasma log10 dilution fold
Vaccination groups and timepoints
WA-1 x2, Day 35
WA-1 x2, Day 127
WA-1 x2 + Omicron x1, Day 140
WA-1 x2 + Omicron x2, Day 148
PBS, Day 35
PBS, Day 127
PBS, Day 140
PBS, Day 148
PBS (n=3 each)
WA-1+Omicron (n=3 each)

Figure S2

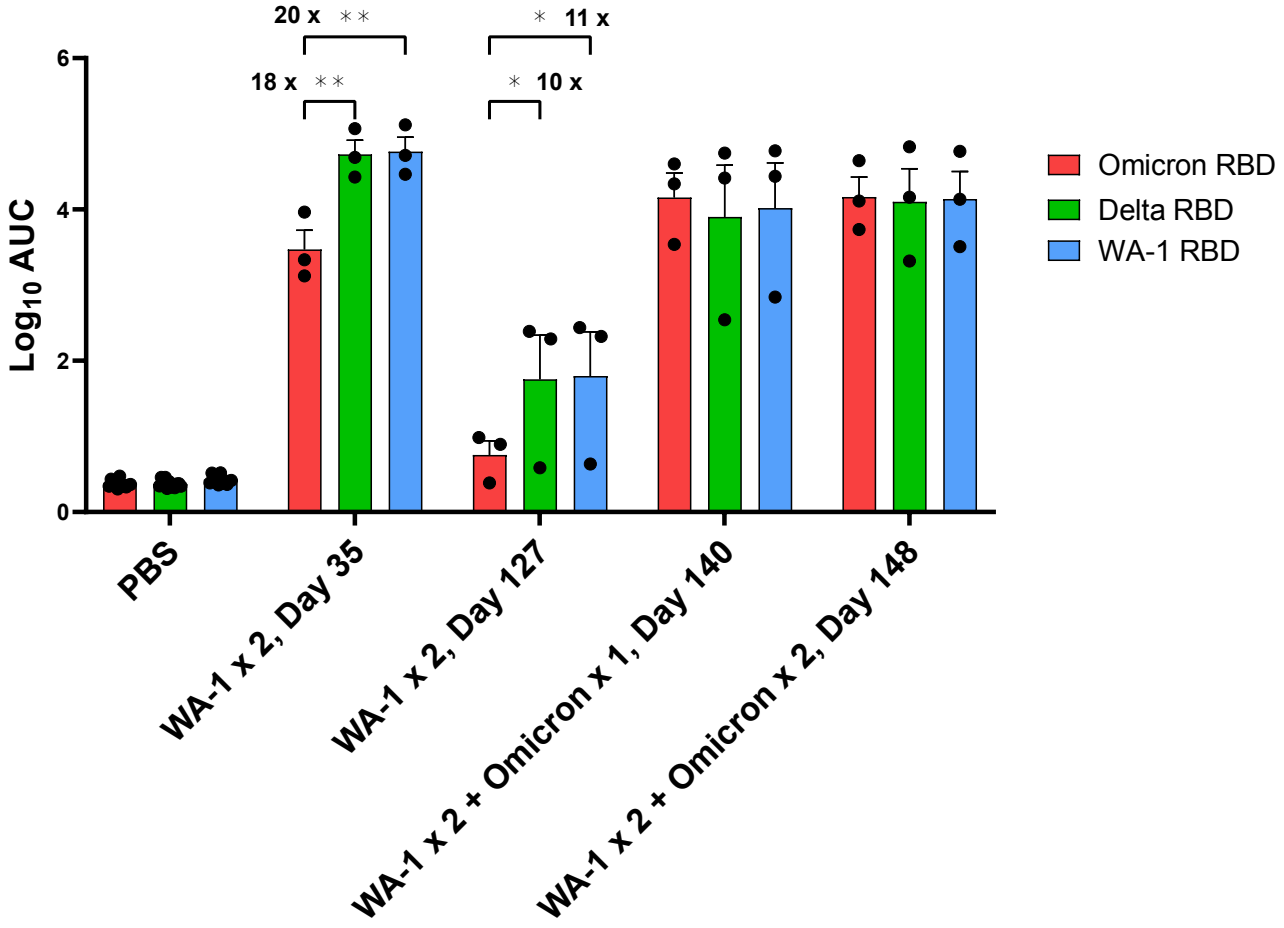
20 x **
18 x **
* 11 x
* 10 x
6
4
2
0
Log10 AUC
PBS
WA-1 x 2, Day 35
WA-1 x 2, Day 127
WA-1 x 2 + Omicron x 1, Day 140
WA-1 x 2 + Omicron x 2, Day 148
Omicron RBD
Delta RBD
WA-1 RBD

Figure S3

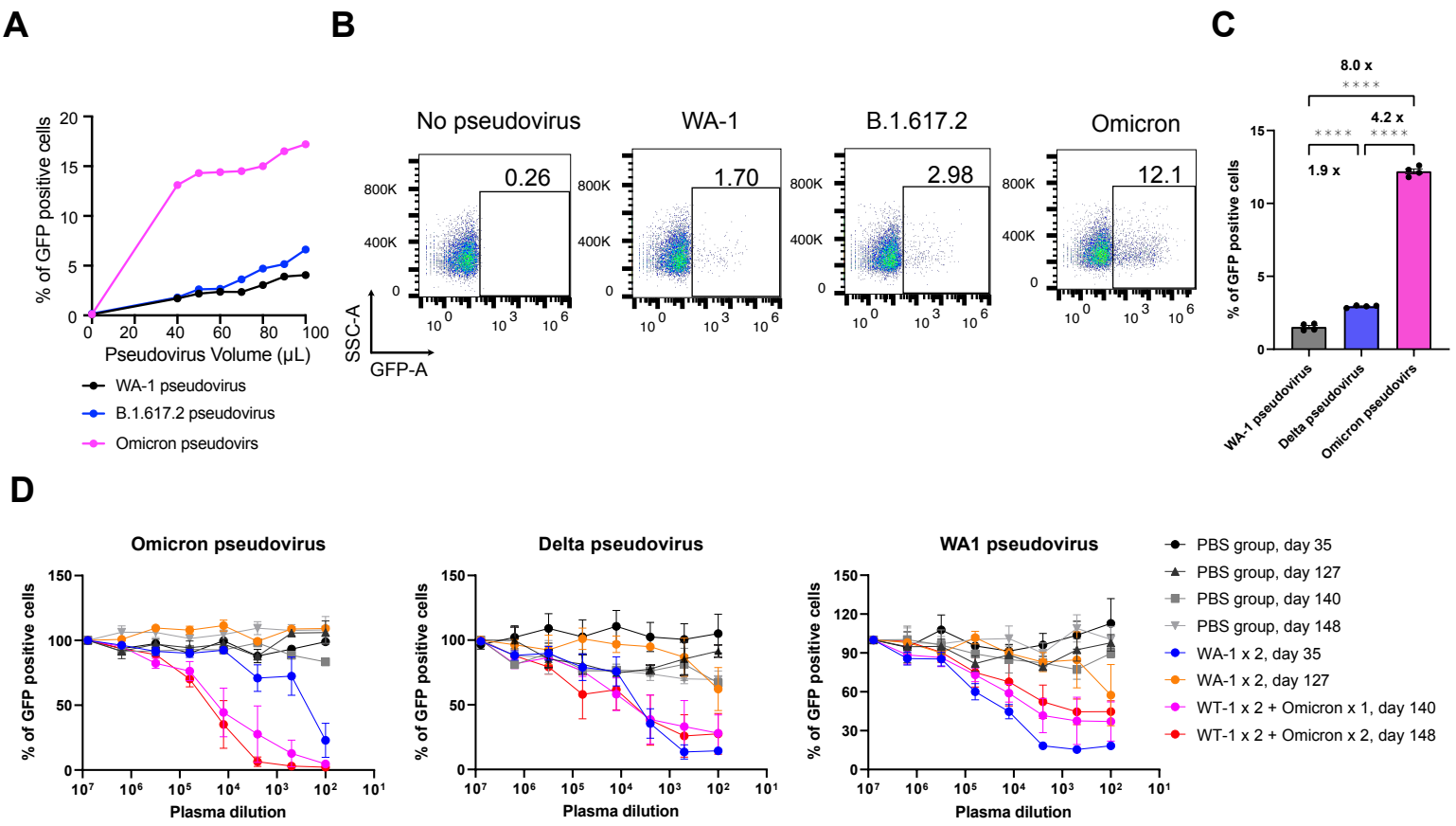
A
% of GFP positive cells
Pseudovirus Volume (μL)
WA-1 pseudovirus
B.1.617.2 pseudovirus
Omicron pseudovirs
B
No pseudovirus
WA-1
B.1.617.2
Omicron
0.26
1.70
2.98
12.1
SSC-A
GFP-A
C
8.0 x
4.2 x
1.9 x
% of GFP positive cells
WA-1 pseudovirus
Delta pseudovirus
Omicron pseudovirs
D
Omicron pseudovirus
Delta pseudovirus
WA1 pseudovirus
% of GFP positive cells
Plasma dilution
PBS group, day 35
PBS group, day 127
PBS group, day 140
PBS group, day 148
WA-1 x 2, day 35
WA-1 x 2, day 127
WT-1 x 2 + Omicron x 1, day 140
WT-1 x 2 + Omicron x 2, day 148

Figure S4

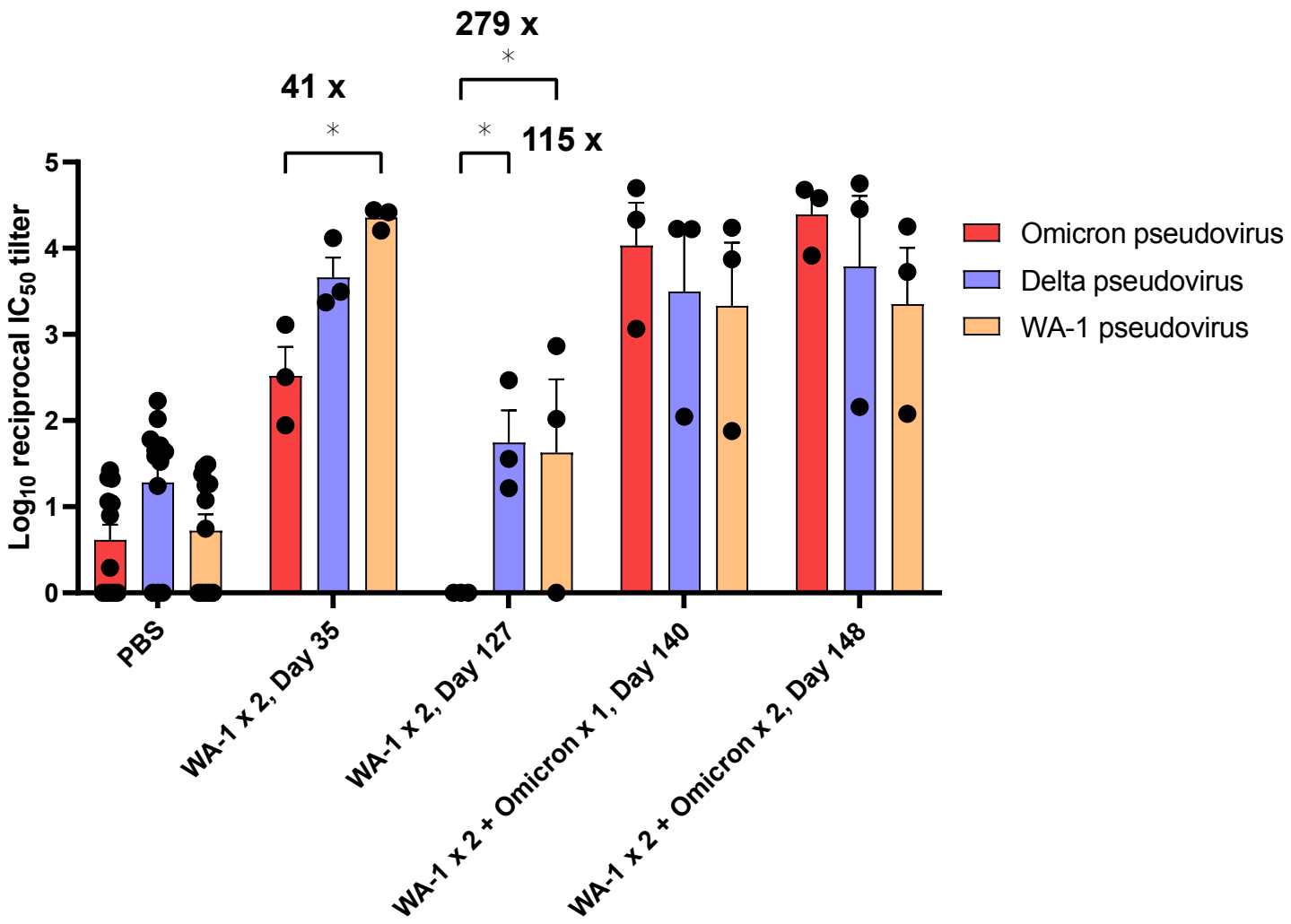
279 x
41 x
115 x
*
*
*
Log10 reciprocal IC50 titer
0
1
2
3
4
5
PBS
WA-1 x 2, Day 35
WA-1 x 2, Day 127
WA-1 x 2 + Omicron x 1, Day 140
WA-1 x 2 + Omicron x 2, Day 148
Omicron pseudovirus
Delta pseudovirus
WA-1 pseudovirus

Figure S5

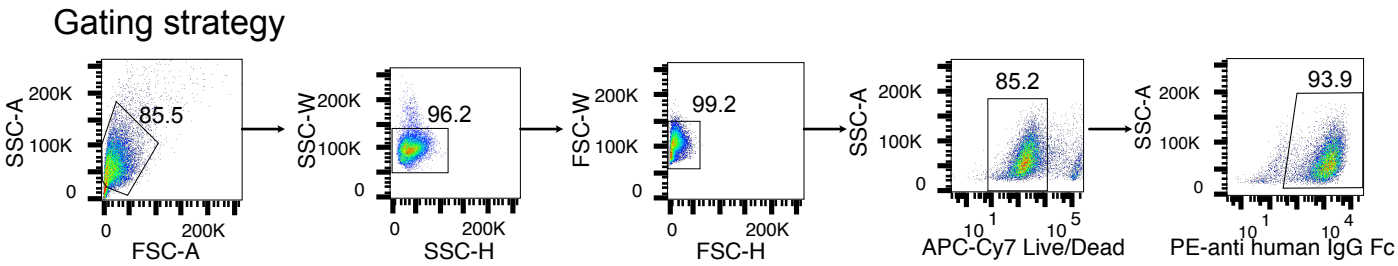
Gating strategy
SSC-A
200K
100K
0
85.5
0
200K
FSC-A
SSC-W
200K
100K
0
96.2
0
200K
SSC-H
FSC-W
200K
100K
0
99.2
0
200K
FSC-H
SSC-A
200K
100K
0
85.2
10 1
10 5
APC-Cy7 Live/Dead
SSC-A
200K
100K
0
93.9
10 1
10 4
PE-anti human IgG Fc